

Supporting Information

From CuFeS₂ to Ba₆Cu₂FeGe₄S₁₆: Rational Band Gap Engineering Achieves Large Second-Harmonic-Generation Together with High Laser Damage Threshold

Wangzhu Cao,^a Dajiang Mei,^{*a} Yi Yang,^{cd} Yuanwang Wu,^e Lingyun Zhang,^a Yuandong Wu,^a Xiao He,^{fg} Zheshuai Lin,^{*cd} and Fuqiang Huang^{*b}

^a College of Chemistry and Chemical Engineering, Shanghai University of Engineering Science, Shanghai 201620, China

*Email: meidajiang718@pku.edu.cn.

^b State Key Laboratory of High Performance Ceramics and Superfine Microstructure, Shanghai Institute of Ceramics, Chinese Academy of Sciences, Shanghai 200050, China

*Email: huangfq@mail.sic.ac.cn.

^c Technical Institute of Physics and Chemistry, Chinese Academy of Sciences, Beijing 100190, China

^d University of Chinese Academy of Sciences, Beijing 100190, China

*Email: zslin@mail.ipc.ac.cn.

^e State Key Laboratory of Bioreactor Engineering, Department of Bioengineering, East China University of Science and Technology, Shanghai, 200237, China

^f Shanghai Engineering Research Center of Molecular Therapeutics and New Drug Development, School of Chemistry and Molecular Engineering, East China Normal University, Shanghai, 200062, China

^g NYU-ECNU Center for Computational Chemistry at NYU Shanghai, Shanghai, 200062, China

Contents

Experimental sections

Figure S1. The experimental and simulated X-ray diffraction result of $\text{Ba}_6\text{Cu}_2\text{FeGe}_4\text{S}_{16}$ powder.

Figure S2. (a) The arrangement of GeS_4 tetrahedrons in the overall structure of $\text{Ba}_6\text{Cu}_2\text{FeGe}_4\text{S}_{16}$ along the $[111]$ direction. (b) The structure of $\text{Ba}_6\text{Cu}_2\text{FeGe}_4\text{S}_{16}$ and the details of the $[\text{Ge}(\text{Cu}/\text{Fe})_3\text{S}_{13}]$ unit. (c) The coordination environment of the Ba atoms.

Figure S3. The SHG intensity of $\text{Ba}_6\text{Cu}_2\text{FeGe}_4\text{S}_{16}$ compared with that of AgGaSe_2 at $2.09 \mu\text{m}$ laser.

Figure S4. The M - T curve of $\text{Ba}_6\text{Cu}_2\text{FeGe}_4\text{S}_{16}$ measured from 5 to 300 K under the applied field $H = 1 \text{ kOe}$. Inset: the $1/M$ - T curve from 5 to 300 K.

Figure S5. DOS and PDOS of $\text{Ba}_6\text{Cu}_2\text{FeGe}_4\text{S}_{16}$.

Table S1. Crystallographic data and refinement details of $\text{Ba}_6\text{Cu}_2\text{FeGe}_4\text{S}_{16}$.

Table S2. Selected bond lengths (\AA) and angles (deg) of $\text{Ba}_6\text{Cu}_2\text{FeGe}_4\text{S}_{16}$.

Experimental sections

Solid-state synthesis

In an argon-protected glove-box, the following purchased reagents, BaS (99.9%), Cu (99.9%), Fe (99.9%), Ge (99.5%), and S (99.99%) were mixed with the molar ratio of 6: 2: 1: 4: 10. Next, the mixed reagents were loaded into the graphic crucible. Then, they were put into the silica tube sealed under vacuum ($<10^{-3}$ Pa) and transferred to a programmed muffle furnace. The sample was heated from room temperature to 1173 K in 24 hours and then there was a 20 hours process of heat preservation. After the temperature was cooled to 573K in 40 hours, the muffle furnace was shut down and the sample was cooled to ambient temperature. The powder X-ray diffraction (XRD) data of $\text{Ba}_6\text{Cu}_2\text{FeGe}_4\text{S}_{16}$ was collected at room temperature using a Bruker D2 X-ray diffractometer equipped with graphite monochromated Cu-K α radiation ($\lambda = 1.5418\text{\AA}$). Besides, the 2θ range of XRD was from 10° to 70° and 0.02° as a scan step width. The experimental XRD data of $\text{Ba}_6\text{Cu}_2\text{FeGe}_4\text{S}_{16}$ powder was compared with the simulated data in Figure S1. And the results showed that the two values are consistent.

Single crystal growth

In an argon-protected glove-box, the prepared $\text{Ba}_6\text{Cu}_2\text{FeGe}_4\text{S}_{16}$ powder was mixed with flux KI at the rate of 1: 1 and then the mixtures were loaded into the graphic crucible. Next, put the graphic crucible into the silica tube and sealed the tube under vacuum ($<10^{-3}$ Pa) and transferred to a programmed muffle furnace. Afterwards, the program temperature was heated to 1173K in 24 hours and maintain at the current temperature for 48 hours, subsequently, the temperature was cooled to 573K in 150 hours. After that, the muffle furnace was shut down and the sample was naturally cooled to ambient temperature. After the sample was taken out, it was cleaned with deionized water to obtain red crystals. The size of single crystal is $0.22\text{mm}\times 0.18\text{mm}\times 0.24\text{mm}$ and these crystals are stable in air.

Crystal structure determination

The single crystal data of target compound $\text{Ba}_6\text{Cu}_2\text{FeGe}_4\text{S}_{16}$ was collected using a Bruker D8 diffractometer equipped with graphite monochromated Mo-K α radiation ($\lambda = 0.71073$). The direct method and the full-matrix least squares method installed on the F² using the SHELX-2016/6 program package¹ were used to solve and refine the single crystal structure.

Diffuse reflectance spectroscopy analysis

In the wavelength range of 200 to 1500 nm, the Shimadzu UV-3600 spectrophotometer was used to test the UV-visible-near infrared diffuse reflectance spectroscopy data of $\text{Ba}_6\text{Cu}_2\text{FeGe}_4\text{S}_{16}$.

Laser damage threshold test

A pulsed YAG laser (1064 nm) was used for LDT testing, meanwhile, a powder sample of AgGaSe_2 with similar size was provided as a reference material.

Second harmonic generation measurement

A 2090 nm Q-switch laser was used to measure the SHG response of the $\text{Ba}_6\text{Cu}_2\text{FeGe}_4\text{S}_{16}$ power sample with particle size of 70-90 μm by Kurtz-Perry method.² At the same time, the reference material was a powder sample of AgGaSe_2 with the same particle size.

Magnetic Moment Measurements

Magnetic moment measurements were recorded using the SQUID tester of Quantum Design with temperature changing from 5 K to 300 K. 40 mg of target compound was placed in the capsules and placed

on the Cu bar for testing, and the pre-squid tester automatically cleared the background signal.

Computational method

The Vienna ab initio simulation package (VASP) code^{3,4} that implements the projector enhanced wave (PAW) pseudopotentials³ was used to calculate the density functional theory (DFT).⁵ In addition, the local density approximation (LDA)^{6,7} is used for exchange-correlation potential. The following electrons were considered as valence electrons: Ba $5s^25p^66s^2$ Fe $3d^64s^2$ Cu $3d^{10}4s^1$ Ge $4s^24p^2$ and S $3s^23p^4$. Kinetic energy (KE) cutoff was 400 eV. In order to optimize the geometry, we used both Monkhorst-Pack 4 k-points and denser 8 k-points (including Gamma points) in the Brillouin zone for DFT and electronic structure calculations respectively. We stopped the geometry optimization when the residual force was less than 0.01 eV/Å and selected the KE cutoff point of 400 eV. The LDA + U method was used to describe the local *d*-orbitals in the Fe and Cu atoms, meanwhile, the on-site orbital dependent Hubbard U energy was set as $U_d = 6$ eV.^{8,9} The calculated energy gaps are 1.8 and 1.2 eV in the spin-up and spin-down directions, respectively.

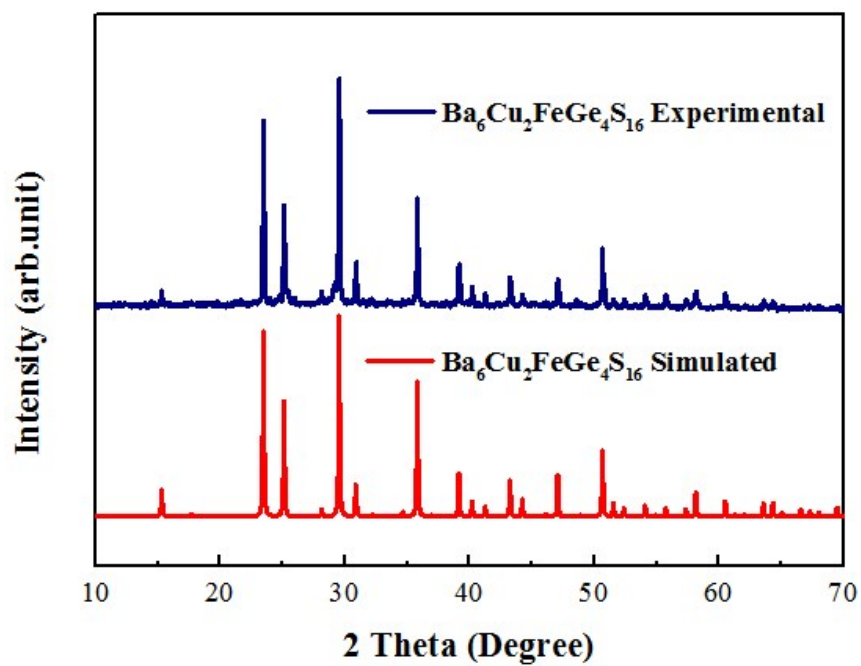


Figure S1. The experimental and simulated X-ray diffraction result of $\text{Ba}_6\text{Cu}_2\text{FeGe}_4\text{S}_{16}$ powder.

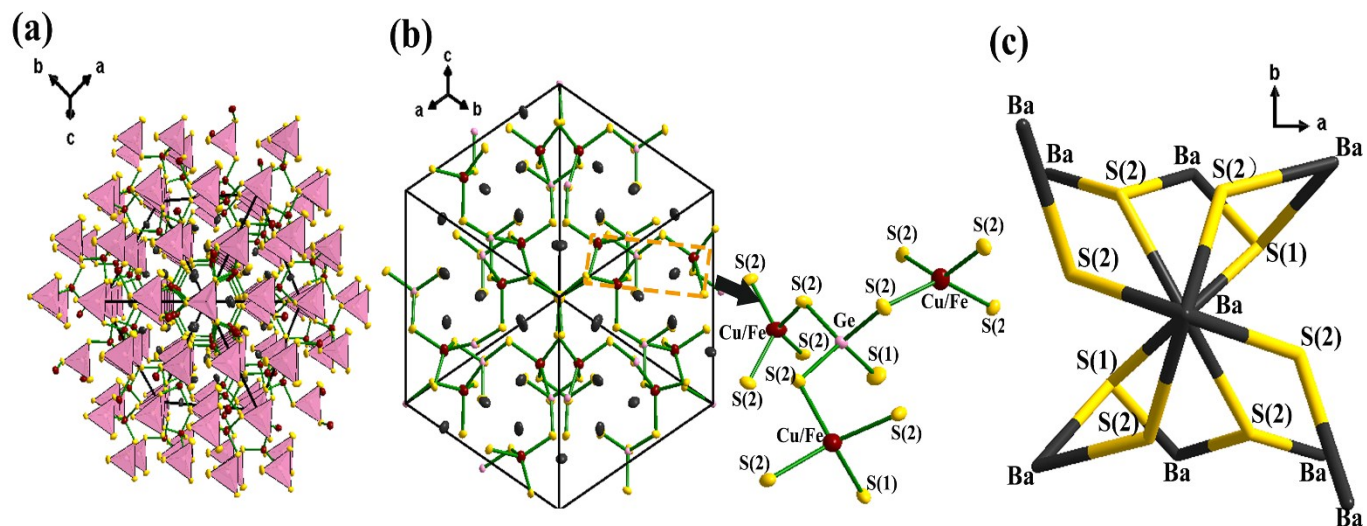


Figure S2. (a) The arrangement of GeS_4 tetrahedrons in the overall structure of $\text{Ba}_6\text{Cu}_2\text{FeGe}_4\text{S}_{16}$ along the $[111]$ direction. (b) The structure of $\text{Ba}_6\text{Cu}_2\text{FeGe}_4\text{S}_{16}$ and the details of the $[\text{Ge}(\text{Cu}/\text{Fe})_3\text{S}_{13}]$ unit. (c) The coordination environment of the Ba atoms.

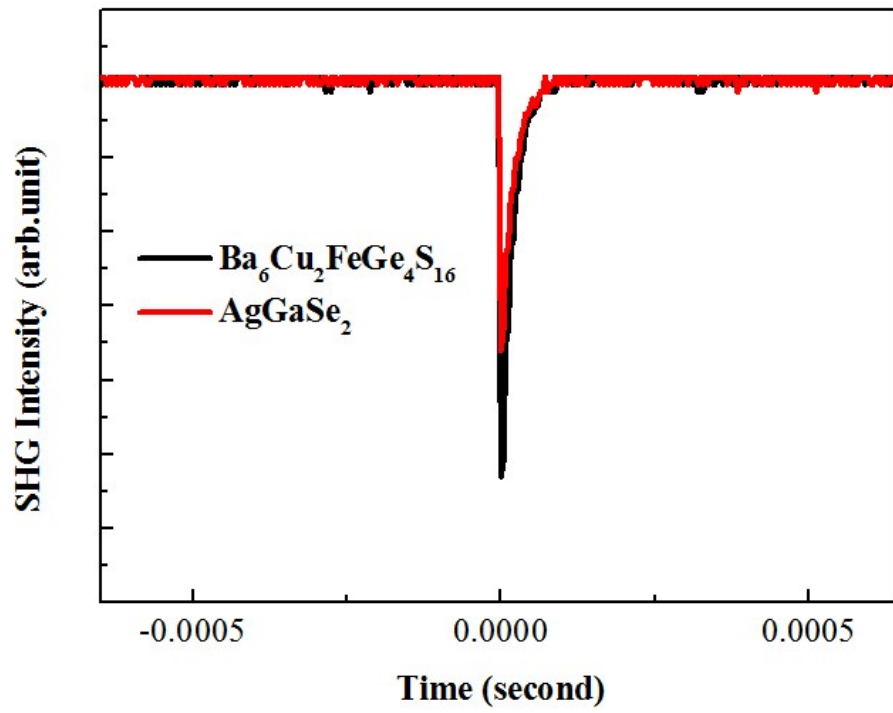


Figure S3. The SHG intensity of $\text{Ba}_6\text{Cu}_2\text{FeGe}_4\text{S}_{16}$ compared with that of AgGaSe_2 at 2.09 μm laser.

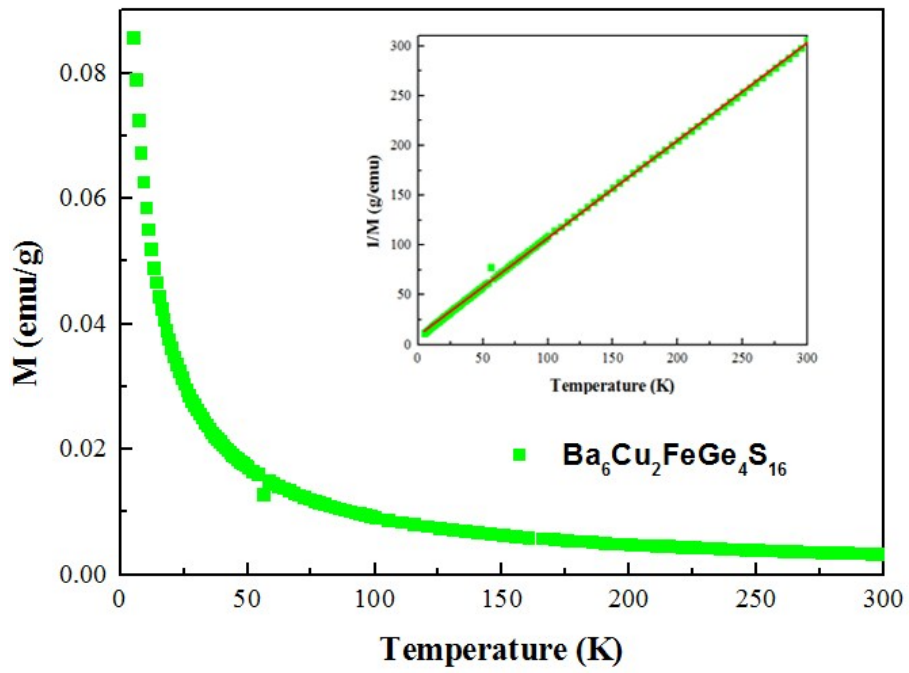


Figure S4. The M - T curve of $\text{Ba}_6\text{Cu}_2\text{FeGe}_4\text{S}_{16}$ measured from 5 to 300 K under the applied field $H = 1$ kOe. Inset: the $1/M$ - T curve from 5 to 300 K.

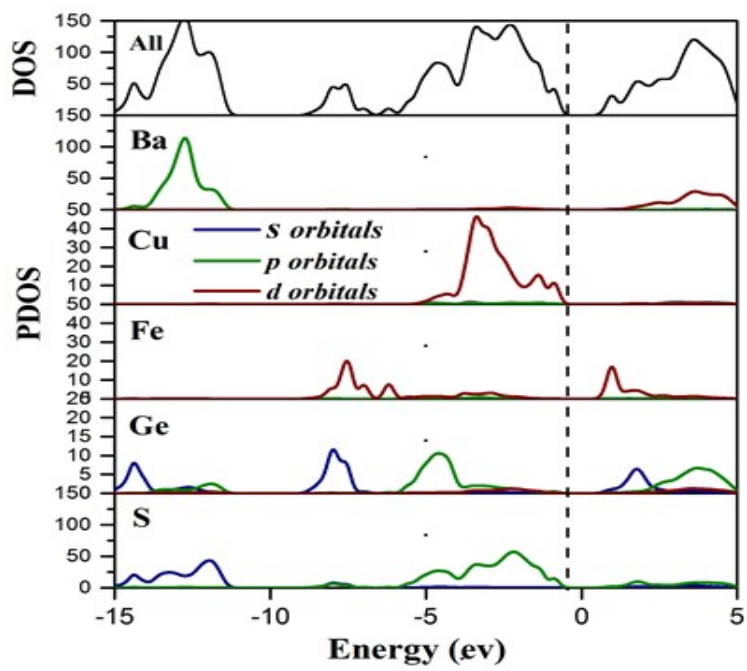


Figure S5. DOS and PDOS of $\text{Ba}_6\text{Cu}_2\text{FeGe}_4\text{S}_{16}$.

Table S1. Crystallographic data and refinement details of Ba₆Cu₂FeGe₄S₁₆.

	Ba ₆ Cu ₂ FeGe ₄ S ₁₆
Fw	1810.29
a (Å)	14.2342 (6)
b (Å)	14.2342 (6)
c (Å)	14.2342 (6)
Volume (Å ³)	2884.0 (4)
Space group	$\bar{I}4_3d$
Z	4
Index ranges	-19 ≤ h ≤ 19 -19 ≤ k ≤ 12 -19 ≤ l ≤ 19
ρ _c (Mg m ⁻³)	4.169
μ (mm ⁻¹)	15.226
R ₁ , wR ₂ [I > 2σ(I)],	0.0297, 0.0701
R ₁ , wR ₂ (all data)	0.0310, 0.0709
Weight = 1 / [sigma ² (F _o ²) + (0.0220 * P) ² + 84.95 * P] where P = (Max (F _o ² , 0) + 2 * F _c ²) / 3	

Table S2. Selected bond lengths (Å) and angles (deg) of Ba₆Cu₂FeGe₄S₁₆.

	Ba ₆ Cu ₂ FeGe ₄ S ₁₆
Ba-S1×2	3.0553(17)
Ba-S2×2	3.237(2)
Ba-S2×2	3.293(2)
Ba-S2×2	3.415(2)
Cu/Fe-S2×4	2.386(2)
Ge-S1×1	2.165(5)
Ge-S2×3	2.227(2)
S2-Cu/Fe-S2×4	99.39(4)
S2-Cu/Fe-S2×2	132.36(11)
S2-Ge-S2×3	108.42(8)
S1-Ge-S2×3	110.50(7)

References

- 1 G. M. Sheldrick, *Acta Cryst.*, 2015, **71**, 3.
- 2 S. K. Kurtz and T. T. Perry, *J. Appl. Phys.*, 1968, **39**, 3798.
- 3 P. E. Blöchl, *Phys. Rev. B*, 1994, **50**, 17953.
- 4 G. Kresse and J. Furthmüller, *Phys. Rev. B*, 1996, **54**, 11169.
- 5 M. C. Payne, M. P. Teter, D. C. Ailan, T. A. Arias and J. D. Joannopoulos, *Rev. Mod. Phys.*, 1992, **64**, 1045.
- 6 D. M. Ceperley and B. J. Alder, *Phys. Rev. Lett.*, 1980, **45**, 566.
- 7 J. P. Perdew and A. Zunger, *Phys. Rev. B*, 1990, **41**, 1227.
- 8 A. Roldán, M. Boronat, A. Corma and F. Illas, *J. Phys. Chem. C*, 2010, **114**, 6511.
- 9 F. H. Elbatal, Y. M. Hamdy and S. Y. Marzouk, *Mater. Chem. Phys.*, 2008, **112**, 991.